

1 Submitted to *Biotechnology and Bioengineering* on xxx

2 Cloning and Characterization of a Panel of Mitochondrial Targeting

3 Sequences for Compartmentalization Engineering in *Saccharomyces*

4 *cerevisiae*

5 Chang Dong^{1,2}, Zhuwei Shi¹, Lei Huang¹, Huimin Zhao^{3*}, Zhinan Xu^{1*}, Jiazhang
6 Lian^{1,2,3*}

7
8 ¹ Key Laboratory of Biomass Chemical Engineering of Ministry of Education, College
9 of Chemical and Biological Engineering, Zhejiang University, Hangzhou 310027,
10 China.

11 ² Hangzhou Global Scientific and Technological Innovation Center, Zhejiang
12 University, Hangzhou 310027, China.

¹³ ³ Department of Chemical and Biomolecular Engineering, University of Illinois at Urbana-Champaign, Urbana, IL 61801, USA.

15

16 * Corresponding authors:

17 Prof. Huimin Zhao (Email: zhao5@illinois.edu)

18 Department of Chemical and Biomolecular Engineering, University of Illinois at
19 Urbana-Champaign, Urbana, IL 61801, USA.

20

21 Prof. Zhinan Xu (E-mail: znxu@zju.edu.cn)

22 Key Laboratory of Biomass Chemical Engineering of Ministry of Education, College
23 of Chemical and Biological Engineering, Zhejiang University, Hangzhou 310027,
24 China

25

26 Prof. Jiazhang Lian (E-mail: jzlian@zju.edu.cn)

27 Key Laboratory of Biomass Chemical Engineering of Ministry of Education, College
28 of Chemical and Biological Engineering, Zhejiang University, Hangzhou 310027,
29 China

30

31 **ABSTRACT**

32 Mitochondrion is generally considered as the most promising subcellular organelle for
33 compartmentalization engineering. Much progress has been made in reconstituting
34 whole metabolic pathways in the mitochondria of yeast to harness the precursor pools
35 (i.e. pyruvate and acetyl-CoA), bypass competing pathways, and minimize
36 transportation limitations. However, only a few mitochondrial targeting sequences
37 (MTSs) have been characterized (i.e. MTS of *COX4*), limiting the application of
38 compartmentalization engineering for multi-gene biosynthetic pathways in the
39 mitochondria of yeast. In the present study, based on the mitochondrial proteome, a
40 total of 18 MTSs were cloned and the efficiency of these MTSs in targeting
41 heterologous proteins, including the *Escherichia coli* FabI and enhanced green
42 fluorescence protein (EGFP) into the mitochondria was evaluated by growth
43 complementation and confocal microscopy. After systematic characterization, seven of
44 the well-performed MTSs were chosen for the colocalization of complete biosynthetic
45 pathways into the mitochondria. As proof of concept, the full α -santalene biosynthetic
46 pathway consisting of 10 genes capable of converting acetyl-coA to α -santalene was
47 compartmentalized into the mitochondria, leading to a 3.7-fold improvement in the
48 production of α -santalene. The newly characterized MTSs should contribute to the
49 expanded metabolic engineering and synthetic biology toolbox for yeast mitochondrial
50 compartmentalization engineering.

51

52 **KEYWORDS:** Mitochondrial targeting sequences, *Saccharomyces cerevisiae*,
53 Compartmentalization engineering, Metabolic engineering, α -Santalene

54

55 **1. INTRODUCTION**

56 *Saccharomyces cerevisiae* is the most well-characterized and widely used model
57 eukaryotic organism and has been developed as a platform cell factory via various
58 metabolic engineering strategies (Borodina and Nielsen 2014; Botstein and Fink 2011;
59 Lian et al. 2018). Its well-characterized genetic background, abundant genetic tools,
60 fast growth rate, and robust fermentation performance are highly conducive to
61 recombinant strain construction and subsequent mass production processes. Numerous
62 high value-added compounds such as artemisinic acid (Ro et al. 2006), thebaine
63 (Galanie et al. 2015), and farnesene (Meadows et al. 2016) have been successfully
64 produced by reconstructing their metabolic pathways in *S. cerevisiae*.

65 While most engineered metabolic pathways are located in the yeast cytoplasm,
66 compartmentalization engineering that redirects the whole metabolic pathways to a
67 subcellular organelle also represents an attractive metabolic engineering strategy. Yeast
68 compartmentalization engineering has demonstrated advantages for the production and
69 accumulation of the desirable compounds in several cases, i.e., reconstructing the
70 synthetic pathway in the endoplasmic reticulum (ER) for morphine or plant terpenoid
71 production (Arendt et al. 2017; Thodey et al. 2014), insulating a toxic enzyme into
72 peroxisome to alleviate cellular toxicity for alkaloid overproduction (Grewal et al.
73 2020), and utilizing the abundant precursors such as pyruvate and acetyl-CoA to
74 synthesize terpenoids in the mitochondria (Farhi et al. 2011; Lv et al. 2016; Yuan and
75 Ching 2016). The various yeast organelles can provide isolated spaces and specific
76 microenvironments that are beneficial for some specific enzymes or pathways in
77 metabolic engineering applications.

78 Mitochondrion, working as the cellular powerhouse (Gray et al. 1999), has been
79 equipped with some unique traits, i.e. carrying their own genetic machinery, containing
80 abundant precursors (such as acetyl-CoA, ATP, NADH, and fatty acyl-AC), and
81 showing a more reducing redox microenvironment with higher pH and lower oxygen
82 concentration (Avalos et al. 2013; Galdieri et al. 2014; Hu et al. 2008; Orij et al. 2009;
83 Schnell et al. 1992). Together with the advantages of higher local enzyme concentration
84 and minimized competing pathways, mitochondrial compartmentalization had been
85 demonstrated to improve the production of various value-added compounds such as
86 valencene (Farhi et al. 2011), isobutanol (Avalos et al. 2013), isoprene (Lv et al. 2016),
87 and amorpha-4,11-diene (Yuan and Ching 2016). To enable mitochondrial
88 compartmentalization, N-terminal mitochondrial targeting sequences (MTSs) are
89 required to relocalize the target enzymes (generally synthesized in the cytoplasm as
90 cytosolic pre-proteins) into the mitochondria. However, only a few MTSs have been
91 characterized, limiting the application of mitochondrial compartmentalization for
92 whole multi-gene biosynthetic pathways. Currently, the MTSs of *COX4* (subunit IV of
93 the cytochrome c oxidase) and *COQ3* (O-methyltransferase in Coenzyme Q
94 biosynthesis) were the best characterized, with the MTS of *COX4* used most frequently
95 for mitochondrial compartmentalization. Although the same MTS could be used
96 repeatedly to localize the whole pathway (i.e. 8 genes of the mevalonate pathway) into
97 the mitochondria (Lv et al. 2016; Yuan and Ching 2016), there are considerable
98 concerns for genome instability with regard to the high recombinant efficiency of *S.*
99 *cerevisiae* and potential competition during the mitochondria importing process.
100 Therefore, systematic characterization of a panel of mitochondrial targeting sequences
101 is highly desirable for expanding the yeast metabolic engineering toolbox for
102 mitochondrial compartmentalization.

103 In the present study, a panel of yeast MTSs were cloned, characterized, and adopted
104 for mitochondrial compartmentalization. Firstly, based on the mitochondrial proteome
105 study, 18 MTSs of the most abundant mitochondrial proteins were chosen and cloned.
106 MTSs were evaluated for their capability to relocalize the *Escherichia coli* FabI protein
107 into the mitochondria of a respiration deficiency strain (*etr1* deletion) for growth
108 complementation. Then, 10 highly active MTSs that restored the cell growth in non-
109 fermentable medium (YPE) were tagged to enhanced green fluorescence protein (EGFP)
110 for fluorescence confocal microscopy analysis. Finally, 6 MTSs with excellent
111 performance were chosen for mitochondrial compartmentalization of multi-gene
112 pathways. As a proof of concept, a total of 10 expression cassettes containing the
113 complete biosynthetic pathway for the conversion of acetyl-CoA to α -santalene were
114 colocalized into the mitochondria, resulting in a 3.7-fold improvement in the production
115 of α -santalene. The newly characterized MTSs should enable the development of
116 sophisticated compartmentalization engineering strategies to harness the yeast
117 mitochondria for the production of high value-added compounds.

118 **2. MATERIALS AND METHODS**

119 **2.1 Strains, cultivation conditions, and reagents**

120 *E. coli* DH5 α was used for plasmid cloning and propagation and recombinant *E.*
121 *coli* strains were cultured with Luria-broth medium supplemented with 100 μ g/mL
122 ampicillin at 37°C. CEN.PK2-1C was the host for growth complementation,
123 fluorescence confocal microscopy analysis, α -santalene pathway assembly, and α -
124 santalene fermentation. Wild type yeast strain was cultured in YPD medium (1% yeast
125 extract, 2% peptone, and 2% glucose). Recombinant yeast strains were maintained in
126 synthetic medium (SCD-LEU and SCD-HIS-URA), containing 1.7 g/L YNB (Difco,

127 Boom, The Netherlands), 5 g/L ammonium sulfate, 20 g/L glucose, and CSM-LEU or
128 CSM-HIS-URA (MP Biomedicals, Solon, Ohio). Growth complementation using non-
129 fermentable carbon source was tested in YPE medium (1% yeast extract, 2% peptone,
130 and 2% ethanol). Q5 polymerase, restriction enzymes, and T4 DNA ligase were
131 purchased from NEB (Ipswich, MA) and all chemicals were purchased from Sigma
132 (Sigma Aldrich, St. Louis, MO) unless stated otherwise.

133 **2.2 Plasmid construction**

134 18 MTSs of the most abundant mitochondrial proteins (Sickmann et al. 2003) were
135 PCR amplified from the genome of CEN.PK2-1C and cloned into the *FabI* expression
136 plasmid pRS425-*ENO2p-NheI-BamHI-FabI-PGK1t*, resulting in the construction of a
137 series of pRS425-*ENO2p*-MTSs-*FabI-PGK1t* plasmids. To visualize the mitochondrial
138 localization via confocal microscope, the selected MTSs were cloned into *EGFP*
139 expression plasmid pH3 (pRS425-*ENO2p-NheI-BamHI-EGFP-PGK1t*). To facilitate
140 the cloning and assembly of mitochondrial targeting pathways, a series of mitochondria
141 helper plasmids (pRS425-promoter-*NheI*-MTSs-*BamHI*-*EGFP*-terminator) were
142 constructed based on the previously developed helper plasmids (Lian and Zhao 2015).
143 For mitochondrial pathway assembly, the mevalonate pathway genes and α -santalene
144 synthase encoding gene were PCR amplified from the yeast genome and pRS425-
145 *SanSyn* (Dong et al. 2020), respectively, and subcloned to the mitochondrial helper
146 plasmids. Individual gene expression cassettes, *GMP1p-MTS1-ERG10-ADH1t*, *GDPP-*
147 *MTS17-MVD1-CYC1t*, *ENO2p-MTS4-ID11-PGK1t*, *TPI1p-MTS8-tHMGR1-TPI1t*,
148 *TEF1p-MTS12-SanSyn-TEF1t*, *GMP1p-MTS1-tHMGR1-ADH1t*, *GDPP-MTS17-*
149 *ERG8-CYC1t*, *ENO2p-MTS4-ERG13-PGK1t*, *TPI1p-MTS12-ERG20-TPI1t*, and
150 *TEF1p-MTS16-ERG12-TEF1t*, were further amplified and assembled with the
151 linearized pRS413 or pRS416 using DNA Assembler (Shao et al. 2009), leading to the

152 construction of two mitochondrial pathway plasmids pRS413-Mito1 and pRS416-
153 Mito2. Yeast plasmids were extracted using the Zymoprep Yeast Plasmid Miniprep II
154 Kit (Zymo Research, Irvine, CA) and amplified in *E. coli*. All plasmids used in this
155 study were listed in Table 1 and oligonucleotides (TSINGKE Biological Technology,
156 Hangzhou, China) used for PCR amplification, plasmid assembly, and diagnostic PCR
157 verification were listed in Supplementary Table S1.

158 **2.3 Strain construction**

159 The *etr1* deficient yeast strain was constructed using the *loxP-KanMX-loxP*
160 method and selected on YPD agar plates supplemented with 200 µg/mL G418. The
161 deletion of the target gene was verified by diagnostic PCR. Yeast strains were
162 transformed using the LiAc/ssDNA/PEG method (Gietz and Schiestl 2007), and
163 transformants were selected on the appropriate selection plates.

164 **2.4 Fluorescence confocal microscopy analysis**

165 Fluorescence visualization and organelle staining were carried out by following the
166 previously established protocols (Baggett et al. 2003) or manufacturer's instructions.
167 For mitochondrial staining, overnight culture was inoculated into 5 mL SCD-LEU
168 medium with an initial OD600 of 0.05, and cultivated at 30°C and 250 rpm for ~18
169 hours when OD600 reached ~0.6-1.0. Mitotracker Red CMXRos (Molecular Probes, 1
170 mM solution in DMSO) was added at a final concentration of 200 nM. The yeast cells
171 were incubated at 30°C (covered with foil, 250 rpm) for 10 min, pelleted, and
172 resuspended in 100 µL phosphate buffer (135 mM NaCl, 2.7 mM KCl, 4.3 mM
173 Na₂HPO₄, and 1.4 mM KH₂PO₄, pH=7.4) with 2% glucose. After staining, cells were
174 mounted onto poly-L-lysine coated slides and visualized using a 63X oil immersion

175 objective lens on a Nikon A1 Confocal Microscope (Nikon, Tokyo, Japan) with an
176 Argon 488 nm laser and a HeNe 543 nm laser.

177 **2.5 α -Santalene fermentation and quantification**

178 α -Santalene producing strains with different combinations of plasmids were pre-
179 cultured in SCD-HIS-URA and inoculated to 5 mL fresh medium with 0.5 ml *n*-
180 dodecane for a two-phase fermentation. After cultivation for 3 days in a 30°C and 250
181 rpm shaker, the supernatant *n*-dodecane layer was collected for α -santalene
182 quantification. 1 μ L diluted sample (with an equal volume of *n*-dodecane, containing
183 caryophyllene as the internal standard) was injected into the SHIMADZU QP2010SE
184 GC-MS system (SHIMADZU, Tokyo, Japan) for analysis, following a previously
185 established protocol (Dong et al. 2020). α -Santalene levels were determined via the
186 internal standard method and normalized to the cell density.

187 **3. RESULTS**

188 **3.1 Selection and cloning of 18 MTSs**

189 The yeast mitochondria harbor a minimized proteome of ~700 proteins (Sickmann
190 et al. 2003). While only a few mitochondria proteins are encoded by the mitochondrial
191 genome, most of the mitochondrial proteins (~95%) are synthesized in the cytosol and
192 redirected to the mitochondria generally with an N-terminal mitochondrial targeting
193 sequence (MTS). Assuming that abundant proteins should have efficient MTSs for
194 mitochondrial targeting, 16 mitochondrial proteins with the highest abundance were
195 selected for subsequent studies in the present study. In addition, the two commonly
196 used MTSs of *COX4* and *COQ3* were included as positive controls. MTSs of the
197 selected proteins were obtained from NCBI annotation as well as predicted by the
198 online tool MITOPROT (<https://ihg.gsf.de/ihg/mitoprot.html>). The longer MTSs were

199 cloned for further characterization, with an additional amino acid (aa) included for
200 MTSSs removal after redirecting the target proteins (Maarse et al. 1984) (Table 2 and
201 Supplementary Table S2).

202 **3.2 Characterization of MTSSs via growth complementation**

203 The mitochondrial targeting efficiency of the selected MTSSs was evaluated by
204 growth complementation of the *etr1* deficient yeast strain on non-fermentable carbon
205 sources (i.e. ethanol and glycerol) via importing its *E. coli* orthologue (FabI) into the
206 mitochondria (Fig. 1A). *ETR1* encodes a mitochondrial 2-enoyl thioester reductase
207 involved in mitochondrial fatty acid biosynthesis, whose deletion resulted in growth
208 failure on non-fermentable carbon sources (Martinez et al. 2004; Torkko et al. 2001).
209 FabI (NADPH-dependent 2-enoyl-acyl carrier protein reductase), the *E. coli* orthologue
210 of Etr1p, should be tagged with MTSSs to complement the growth of the *etr1* deletion
211 strain (Torkko et al. 2001). Therefore, the 18 selected MTSSs were cloned into the *FabI*
212 expression plasmid pRS425-*ENO2p-BamHI-FabI-PGK1t* and the resultant plasmids
213 were transformed into the *etr1* null strain, followed by the evaluation of the growth on
214 non-fermentable medium YPE. As shown in Figure 1B, all strains showed cell growth
215 recovery although to different degrees when compared with the negative control strain
216 (expressing FabI in the cytosol of yeast), indicating all MTSSs were able to redirect FabI
217 into the mitochondria with various efficiencies. MTS1, MTS3, MTS4, MTS8, MTS9,
218 MTS10, MTS12, MTS16, MTS17, and MTS18 enabled the best growth
219 complementation and were selected for further characterization.

220 **3.3 Characterization of selected MTSSs via confocal microscopy analysis**

221 After the growth complementation assays, the selected MTSSs were further
222 characterized via fluorescence confocal microscopy. Thus, the selected MTSSs were

223 cloned into *EGFP* expression plasmid pH3 (pRS425-*ENO2p-BamHI-EGFP-PGK1t*).
224 A yeast strain expressing cytosolic EGFP was included as a negative control.
225 Fluorescence distribution of EGFP was visualized using a fluorescence confocal
226 microscope and a MitoTracker Red dye was used to indicate the location of
227 mitochondria. As shown in Fig. 2, the fluorescence of EGFP was highly condensed and
228 matched the location of the mitochondria for MTS1, MTS4, MTS8, MTS9, MTS12,
229 MTS16, and MTS17, while the fluorescence was distributed in both cytoplasm and
230 mitochondria for MTS3, MTS10, and MTS18. These results indicated that MTS1,
231 MTS4, MTS8, MTS9, MTS12, MTS16, and MTS17 were able to import most of EGFP
232 to the mitochondria, while MTS3, MTS10, and MTS18 only enabled partial
233 mitochondrial targeting. Considering the high efficiency in redirecting both FabI and
234 EGFP to the mitochondria, MTS1, MTS4, MTS8, MTS9, MTS12, MTS16, and MTS17
235 could be used for mitochondrial compartmentalization of the whole multi-gene
236 biosynthetic pathways.

237 **3.4 Mitochondrial compartmentalization of the whole α -santalene biosynthetic
238 pathway using multiple MTSs**

239 Finally, compartmentalization of a complete metabolic pathway into the
240 mitochondria was attempted using the multiple MTSs characterized in the present study.
241 To facilitate the assembly of multi-MTS-gene pathways, six mitochondrial helper
242 plasmids (pMH101, pMH102, pMH103, pMH104, pMH105, and pMH106, harboring
243 MTS1, MTS17, MTS4, MTS8, MTS12, and MTS16, respectively) were constructed,
244 based on the previously developed helper plasmids (Lian and Zhao 2015). Using the
245 additional promoters or terminators as the homologous recombination arms, multi-
246 MTS-gene pathways can be constructed in a single step using via the DNA Assembler
247 method (Shao et al. 2009).

248 To demonstrate the utility of these characterized MTSs and helper plasmids for
249 mitochondria compartmentalization engineering, the mevalonate (MVA) pathway and
250 the α -santalene biosynthesis pathway were reconstituted to enable the conversion of
251 acetyl-CoA to α -santalene in the yeast mitochondria. The yeast MVA pathway is
252 located in the cytosol (Kuzuyama and Seto 2012) and responsible for producing the
253 important precursor, farnesyl pyrophosphate (FPP), for the synthesis of numerous
254 terpenoid compounds. α -Santalene is a plant sesquiterpene synthesized from FPP by a
255 santalene synthase (*SanSyn*) and serves as the intermediate for the biosynthesis of
256 santalol (an important traditional medicine and perfumery ingredient) (Scalcani et al.
257 2012). FPP could be translocated from the cytosol into the mitochondria, which had
258 been proved to be a limiting step for subsequent conversions (Farhi et al. 2011; Yuan
259 and Ching 2016). By relocating the whole MVA pathway into the mitochondria with
260 abundant acetyl-CoA supply, α -santalene production should be significantly improved.
261 The complete MVA pathway genes (*ERG10*, *ERG13*, *tHMGR*, *ERG12*, *ERG8*, *ERG19*,
262 *ID11*, and *ERG20*) and the α -santalene synthase gene (*SanSyn*) were cloned into the
263 mitochondrial helper plasmids (pMH101–pMH105) (Table 2). As *tHMGR* has been
264 determined to be the rate-limiting enzyme, two copies of MTS-*tHMGR* were included
265 in two separate plasmids (pRS413-Mito1 and pRS416-Mito2, Table1).

266 The α -santalene production level was evaluated in recombinant strains harboring
267 different combinations of plasmids using two-phase fermentation. As showed in Fig.3,
268 the targeting of *SanSyn* into mitochondria resulted in a 50% decrease in the production
269 level of α -santalene, indicating that the supply of FPP might be limiting in the
270 mitochondria. The compartmentalization of the full MVA pathway into mitochondria
271 significantly enhanced FPP supply and accordingly the production level of α -santalene
272 was increased by more than 3.7-fold. The compartmentalization of a partial MVA

273 pathway (p416-Mito2) had no effect on the production level of α -santalene, indicating
274 that the full MVA pathway was required for the synthesis of FPP from acetyl-CoA in
275 the yeast mitochondria. Considering that most of the enzymes and intermediates of the
276 MVA pathway were absent in the yeast mitochondria, the enhancement of α -santalene
277 production by the complete pathway but not the incomplete pathway indicated that all
278 the enzymes of the full pathway were successfully compartmentalized into the
279 mitochondria.

280 **5. DISCUSSION**

281 In this study, a total of 18 MTSs were cloned and evaluated via growth
282 complementation and fluorescence confocal microscopy analysis. Seven MTSs
283 demonstrated excellent performance in targeting both the *E. coli* FabI and EGFP to the
284 mitochondria, indicating their potential application in the compartmentalization of
285 other heterologous proteins or pathways into the mitochondria. In addition, a series of
286 mitochondrial helper plasmids (pMH101-pMH106, Table 1) were constructed to
287 facilitate the assembly of multi-MTS-gene pathways for metabolic engineering and
288 synthetic biology applications. As a proof of concept, the complete MVA pathway and
289 the α -santalene synthesis pathway were compartmentalized into the yeast mitochondria,
290 leading to ~4-fold improvement in the production of α -santalene.

291 The *E. coli* FabI tagged with the 18 MTSs could recover the growth of the *etr1*
292 deficient strain to various degrees, indicating their difference in the mitochondrial
293 targeting efficiency for heterologous proteins. Notably, MTS18 (MTS of *COQ3*) was
294 commonly used in previous studies to either simply relocate proteins into the
295 mitochondria (Gurvitz 2009; Hsu et al. 1996) or enable mitochondrial
296 compartmentalization of multi-gene pathways (Yuan and Ching 2016). However,
297 MTS18 was found to relocate FabI and EGFP to the mitochondria at a much lower

298 efficiency than those characterized in the present study (i.e. MTS1, MTS4, MTS8,
299 MTS9, MTS12, MTS16, and MTS17) and should be excluded in future
300 compartmentalization engineering studies.

301 In the proof-of-concept study, the targeting of SanSyn to the mitochondria turned
302 out to lower the α -santalene production level, when compared with the untagged
303 SanSyn in the cytosol (Fig. 3B). In previous studies, the amorpha-4,11-diene
304 production level was significantly improved when relocating the amorpha-4,11-diene
305 synthase (ADS) into the mitochondria (Farhi et al. 2011), while the isoprene
306 productivity was lower with mitochondrially targeted isoprene synthase (ISPS) (Lv et
307 al. 2016). The discrepancy in the effects of mitochondrial targeting on the production
308 level might result from the unique microenvironment of the mitochondria matrix, which
309 was favorable for some proteins (Blumhoff et al. 2013; Farhi et al. 2011). In other words,
310 the effects of compartmentalization on heterologous enzyme activities or terpenoid
311 production levels should be evaluated case by case.

312 In conclusion, a panel of MTSs was systematically characterized for the first time,
313 many of which demonstrated excellent mitochondria targeting performance. Together
314 with the constructed mitochondrial helper plasmids, a metabolic engineering toolbox
315 was established to facilitate fast assembly and efficient colocalization of a full pathway
316 into the mitochondria. This study should contribute to the fast-developing
317 compartmentalization engineering to harness the unique microenvironment of the
318 mitochondrial matrix and the abundant mitochondria acetyl-CoA pool.

319 **ACKNOWLEDGMENTS**

320 This work was supported by the National Key Research and Development Program of
321 China (2018YFA0901800 to JL), the Natural Science Foundation of China (21808199

322 to JL), the Natural Science Foundation of Zhejiang Province (R20B060006 to JL), and
323 the U.S. Department of Energy, Office of Science, Office of Biological and
324 Environmental Research (DE-SC0018420 to HZ).

325 **AUTHOR CONTRIBUTIONS**

326 J.L. and H.Z. conceived the study. C.D., Z.S., and J.L. performed the experiments. C.D.
327 drafted the manuscript. L.H., J.L., Z.X., and H.Z. revised the manuscript. All authors
328 approved the manuscript.

329 **SUPPORTING INFORMATION**

330 Additional Supporting Information may be found online in the supporting information
331 tab for this article.

332 **REFERENCES**

333 Arendt P, Miettinen K, Pollier J, De Rycke R, Callewaert N, Goossens A. 2017. An endoplasmic
334 reticulum-engineered yeast platform for overproduction of triterpenoids. *Metabolic*
335 *Engineering* 40:165-175.

336 Avalos JL, Fink GR, Stephanopoulos G. 2013. Compartmentalization of metabolic pathways in yeast
337 mitochondria improves the production of branched-chain alcohols. *Nature Biotechnology*
338 31(4):335-41.

339 Baggett JJ, Shaw JD, Sciambi CJ, Watson HA, Wendland B. 2003. Fluorescent labeling of yeast. *Current*
340 *Protocols in Cell Biology* Chapter 4:Unit 4 13.

341 Blumhoff ML, Steiger MG, Mattanovich D, Sauer M. 2013. Targeting enzymes to the right compartment:
342 metabolic engineering for itaconic acid production by *Aspergillus niger*. *Metabolic Engineering*
343 19:26-32.

344 Borodina I, Nielsen J. 2014. Advances in metabolic engineering of yeast *Saccharomyces cerevisiae* for
345 production of chemicals. *Biotechnology Journal* 9(5):609-20.

346 Botstein D, Fink GR. 2011. Yeast: an experimental organism for 21st Century biology. *Genetics*
347 189(3):695-704.

348 Dong C, Jiang L, Xu S, Huang L, Cai J, Lian J, Xu Z. 2020. A single Cas9-VPR nuclease for simultaneous
349 gene activation, repression, and editing in *Saccharomyces cerevisiae*. *ACS Synthetic Biology*
350 9(9):2252-2257.

351 Farhi M, Marhevka E, Masci T, Marcos E, Eyal Y, Ovadis M, Abeliovich H, Vainstein A. 2011.
352 Harnessing yeast subcellular compartments for the production of plant terpenoids. *Metabolic*
353 *Engineering* 13(5):474-81.

354 Galanis S, Thodey K, Trenchard IJ, Filsinger Interrante M, Smolke CD. 2015. Complete biosynthesis of
355 opioids in yeast. *Science* 349(6252):1095-100.

356 Galdieri L, Zhang T, Rogerson D, Lleshi R, Vancura A. 2014. Protein acetylation and acetyl coenzyme
357 a metabolism in budding yeast. *Eukaryotic Cell* 13(12):1472-83.

358 Gietz RD, Schiestl RH. 2007. High-efficiency yeast transformation using the LiAc/SS carrier DNA/PEG
359 method. *Nature Protocols* 2(1):31-4.

360 Gray MW, Burger G, Lang BF. 1999. Mitochondrial evolution. *Science* 283(5407):1476-81.

361 Grewal PS, Samson JA, Baker JJ, Choi B, Dueber JE. 2020. Peroxisome compartmentalization of a toxic
362 enzyme improves alkaloid production. *Nature Chemical Biology*.

363 Gurvitz A. 2009. The essential mycobacterial genes, fabG1 and fabG4, encode 3-oxoacyl-thioester
364 reductases that are functional in yeast mitochondrial fatty acid synthase type 2. *Molecular*
365 *Genetics and Genomics* 282(4):407-16.

366 Hsu AY, Poon WW, Shepherd JA, Myles DC, Clarke CF. 1996. Complementation of coq3 mutant yeast
367 by mitochondrial targeting of the *Escherichia coli* UbiG polypeptide: evidence that UbiG
368 catalyzes both O-methylation steps in ubiquinone biosynthesis. *Biochemistry* 35(30):9797-806.

369 Hu J, Dong L, Outten CE. 2008. The redox environment in the mitochondrial intermembrane space is
370 maintained separately from the cytosol and matrix. *Journal of Biological Chemistry*
371 283(43):29126-34.

372 Kuzuyama T, Seto H. 2012. Two distinct pathways for essential metabolic precursors for isoprenoid
373 biosynthesis. *Proceedings of the Japan Academy, Series B* 88(3):41-52.

374 Lian J, Hamedirad M, Zhao H. 2018. Advancing metabolic engineering of *Saccharomyces cerevisiae*
375 using the CRISPR/Cas system. *Biotechnology Journal* 13(9):1700601.

376 Lian J, Zhao H. 2015. Reversal of the beta-oxidation cycle in *Saccharomyces cerevisiae* for production
377 of fuels and chemicals. *ACS Synthetic Biology* 4(3):332-41.

378 Lv X, Wang F, Zhou P, Ye L, Xie W, Xu H, Yu H. 2016. Dual regulation of cytoplasmic and
379 mitochondrial acetyl-CoA utilization for improved isoprene production in *Saccharomyces cerevisiae*.
380 *Nature Communications* 7:12851.

381 Maarse AC, Van Loon AP, Riezman H, Gregor I, Schatz G, Grivell LA. 1984. Subunit IV of yeast
382 cytochrome c oxidase: cloning and nucleotide sequencing of the gene and partial amino acid
383 sequencing of the mature protein. *The EMBO Journal* 3(12):2831-7.

384 Martinez MJ, Roy S, Archuleta AB, Wentzell PD, Anna-Arriola SS, Rodriguez AL, Aragon AD,
385 Quinones GA, Allen C, Werner-Washburne M. 2004. Genomic analysis of stationary-phase and
386 exit in *Saccharomyces cerevisiae*: Gene expression and identification of novel essential genes.
387 *Molecular Biology of the Cell* 15(12):5295-305.

388 Meadows AL, Hawkins KM, Tsegaye Y, Antipov E, Kim Y, Raetz L, Dahl RH, Tai A, Mahatdejkul-
389 Meadows T, Xu L and others. 2016. Rewriting yeast central carbon metabolism for industrial
390 isoprenoid production. *Nature* 537(7622):694-697.

391 Orij R, Postmus J, Ter Beek A, Brul S, Smits GJ. 2009. In vivo measurement of cytosolic and
392 mitochondrial pH using a pH-sensitive GFP derivative in *Saccharomyces cerevisiae* reveals a
393 relation between intracellular pH and growth. *Microbiology (Reading)* 155(Pt 1):268-278.

394 Ro DK, Paradise EM, Ouellet M, Fisher KJ, Newman KL, Ndungu JM, Ho KA, Eachus RA, Ham TS,
395 Kirby J and others. 2006. Production of the antimalarial drug precursor artemisinic acid in
396 engineered yeast. *Nature* 440(7086):940-3.

397 Scalcinati G, Knuf C, Partow S, Chen Y, Maury J, Schalk M, Daviet L, Nielsen J, Siewers V. 2012.
398 Dynamic control of gene expression in *Saccharomyces cerevisiae* engineered for the production
399 of plant sesquiterpene alpha-santalene in a fed-batch mode. *Metabolic Engineering* 14(2):91-
400 103.

401 Schnell N, Krems B, Entian KD. 1992. The PAR1 (YAP1/SNQ3) gene of *Saccharomyces cerevisiae*, a
402 c-jun homologue, is involved in oxygen metabolism. *Current Genetics* 21(4-5):269-73.

403 Shao Z, Zhao H, Zhao H. 2009. DNA assembler, an *in vivo* genetic method for rapid construction of
404 biochemical pathways. *Nucleic Acids Research* 37(2):e16.

405 Sickmann A, Reinders J, Wagner Y, Joppich C, Zahedi R, Meyer HE, Schonfisch B, Perschil I,
406 Chacinska A, Guiard B and others. 2003. The proteome of *Saccharomyces cerevisiae*
407 mitochondria. *Proceedings of the National Academy of Sciences of the United States of America*
408 100(23):13207-12.

409 Thodey K, Galanis S, Smolke CD. 2014. A microbial biomanufacturing platform for natural and
410 semisynthetic opioids. *Nature Chemical Biology* 10(10):837-44.

411 Torkko JM, Koivuranta KT, Miinalainen IJ, Yagi AI, Schmitz W, Kastaniotis AJ, Airenne TT, Gurvitz
412 A, Hiltunen KJ. 2001. Candida tropicalis Etr1p and *Saccharomyces cerevisiae* Ybr026p
413 (Mrfl'p), 2-enoyl thioester reductases essential for mitochondrial respiratory competence.
414 *Molecular and Cellular Biology* 21(18):6243-53.

415 Yuan J, Ching CB. 2016. Mitochondrial acetyl-CoA utilization pathway for terpenoid productions.
416 *Metabolic Engineering* 38:303-309.

417

418 **Table 1.** List of plasmids used in this study

Name	Description	Reference
pRS413	<i>HIS3</i> marker with CEN/ARS4 origin	This lab
pRS416	<i>URA3</i> marker with CEN/ARS4 origin	This lab
pMTS1-FABI	pRS425- <i>ENO2p-MTS1-FabI-PGK1t</i>	This study
pMTS2-FABI	pRS425- <i>ENO2p-MTS2-FabI-PGK1t</i>	This study
pMTS3-FABI	pRS425- <i>ENO2p-MTS3-FabI-PGK1t</i>	This study
pMTS4-FABI	pRS425- <i>ENO2p-MTS4-FabI-PGK1t</i>	This study
pMTS5-FABI	pRS425- <i>ENO2p-MTS5-FabI-PGK1t</i>	This study
pMTS6-FABI	pRS425- <i>ENO2p-MTS6-FabI-PGK1t</i>	This study
pMTS7-FABI	pRS425- <i>ENO2p-MTS7-FabI-PGK1t</i>	This study
pMTS8-FABI	pRS425- <i>ENO2p-MTS8-FabI-PGK1t</i>	This study
pMTS9-FABI	pRS425- <i>ENO2p-MTS9-FabI-PGK1t</i>	This study
pMTS10-FABI	pRS425- <i>ENO2p-MTS10-FabI-PGK1t</i>	This study
pMTS11-FABI	pRS425- <i>ENO2p-MTS11-FabI-PGK1t</i>	This study
pMTS12-FABI	pRS425- <i>ENO2p-MTS12-FabI-PGK1t</i>	This study
pMTS13-FABI	pRS425- <i>ENO2p-MTS13-FabI-PGK1t</i>	This study
pMTS14-FABI	pRS425- <i>ENO2p-MTS14-FabI-PGK1t</i>	This study
pMTS15-FABI	pRS425- <i>ENO2p-MTS15-FabI-PGK1t</i>	This study
pMTS16-FABI	pRS425- <i>ENO2p-MTS16-FabI-PGK1t</i>	This study
pMTS17-FABI	pRS425- <i>ENO2p-MTS17-FabI-PGK1t</i>	This study
pMTS18-FABI	pRS425- <i>ENO2p-MTS18-FabI-PGK1t</i>	This study
pMTS1-EGFP	pRS425- <i>ENO2p-MTS1-EGFP-PGK1t</i>	This study
pMTS3-EGFP	pRS425- <i>ENO2p-MTS3-EGFP-PGK1t</i>	This study
pMTS4-EGFP	pRS425- <i>ENO2p-MTS4-EGFP-PGK1t</i>	This study
pMTS8-EGFP	pRS425- <i>ENO2p-MTS8-EGFP-PGK1t</i>	This study
pMTS9-EGFP	pRS425- <i>ENO2p-MTS9-EGFP-PGK1t</i>	This study
pMTS10-EGFP	pRS425- <i>ENO2p-MTS10-EGFP-PGK1t</i>	This study
pMTS12-EGFP	pRS425- <i>ENO2p-MTS12-EGFP-PGK1t</i>	This study
pMTS16-EGFP	pRS425- <i>ENO2p-MTS16-EGFP-PGK1t</i>	This study
pMTS17-EGFP	pRS425- <i>ENO2p-MTS17-EGFP-PGK1t</i>	This study
pMTS18-EGFP	pRS425- <i>ENO2p-MTS18-EGFP-PGK1t</i>	This study
pMH101	pRS425- <i>GMP1p-NheI-MTS1-BamHI-EGFP-XhoI-PYK1t</i>	This study
pMH102	pRS425- <i>4yrl-ADH1t-GPDp-NheI-MTS17-BamHI-EGFP-XhoI-CYC1t-SbfI-ENO2p</i>	This study
pMH103	pRS425- <i>SbfI-ENO2p-NheI-MTS4-BamHI-EGFP-XhoI-PGK1t-NotI-TPI1p</i>	This study
pMH104	pRS425- <i>NotI-TPI1p-NheI-MTS8-BamHI-EGFP-XhoI-TPI1t-SacII-TEF1p</i>	This study
pMH105	pRS425- <i>SacII-TEF1p-NheI-MTS12-BamHI-EGFP-XhoI-TEF1t-XmaI</i>	This study
pMH106	pRS425- <i>TEF1t-PGK1p-NheI-MTS16-BamHI-EGFP-HindIII-HXT7t</i>	This study
pERG10mt	pMH101- <i>ERG10</i>	This study
pMVD1mt	pMH102- <i>MVD1</i>	This study
pIDI1mt	pMH103- <i>IDII</i>	This study

ptHMGR1mt	pMH104- <i>tHMGR</i>	This study
pSanSynmt	pMH105- <i>SanSyn</i>	This study
ptHMGR2mt	pMH101- <i>tHMGR</i>	This study
pERG8mt	pMH102- <i>ERG8</i>	This study
pERG13mt	pMH103- <i>ERG13</i>	This study
pERG20mt	pMH104- <i>ERG20</i>	This study
pERG12mt	pMH105- <i>ERG12</i>	This study
pRS413-Mito1	pRS413- <i>GMP1p-MTS1-ERG10-PYK1t-GPDp-MTS17-MVD1-CYC1t-ENO2p-MTS4-ID11-PGK1t-TPI1p-MTS8-tHMGR-TPI1t-TEF1p-MTS12-SanSyn-TEF1t</i>	This study
pRS413-Mito2	pRS416- <i>GMP1p-MTS1-tHMGR-PYK1t-GPDp-MTS17-ERG8-CYC1t-ENO2p-MTS4-ERG13-PGK1t-TPI1p-MTS8-ERG20-TPI1t-TEF1p-MTS12-ERG12-TEF1t</i>	This study
pRS413-SanSyn	pRS413- <i>TEF1p-SanSyn-TEF1t</i>	This study
pRS413-SanSynmt	pRS413- <i>TEF1p-MTS12-SanSyn-TEF1t</i>	This study

419

420 **Table 2.** Mitochondrial targeting sequences (MTSs) cloned for characterization

MTS	Target Genes	Predicted Targeting Sequences		Cloned for Characterization
		NCBI	MITOPROT	
MTS1	<i>MMF1</i>	1-17 aa	1-25 aa	1-26 aa
MTS2	<i>HSP10</i>	NA	1-26 aa	1-27 aa
MTS3	<i>SOD2</i>	1-26 aa	1-26 aa	1-27 aa
MTS4	<i>HSP60</i>	1-25 aa	1-22 aa	1-26 aa
MTS5	<i>SSC1</i>	1-23 aa	1-23 aa	1-24 aa
MTS6	<i>KGD2</i>	NA	1-71 aa	1-72 aa
MTS7	<i>LAT1</i>	1-28 aa	1-28 aa	1-29 aa
MTS8	<i>LSC2</i>	NA	1-38 aa	1-39 aa
MTS9	<i>ALD4</i>	1-24 aa	1-31 aa	1-32 aa
MTS10	<i>ACO1</i>	NA	1-23 aa	1-24 aa
MTS11	<i>CIT1</i>	1-37 aa	1-37 aa	1-38 aa
MTS12	<i>LPD1</i>	1-21 aa	1-28 aa	1-29 aa
MTS13	<i>ILV5</i>	1-47 aa	1-34 aa	1-48 aa
MTS14	<i>ADH3</i>	1-27 aa	1-24 aa	1-28 aa
MTS15	<i>IDH2</i>	1-15 aa	1-26 aa	1-27 aa
MTS16	<i>MDH1</i>	1-17 aa	1-17 aa	1-18 aa
MTS17	<i>COX4</i>	1-25 aa	1-25 aa	1-26 aa
MTS18	<i>COQ3</i>	1-32 aa	1-31 aa	1-33 aa

421

422 **Figure legends**

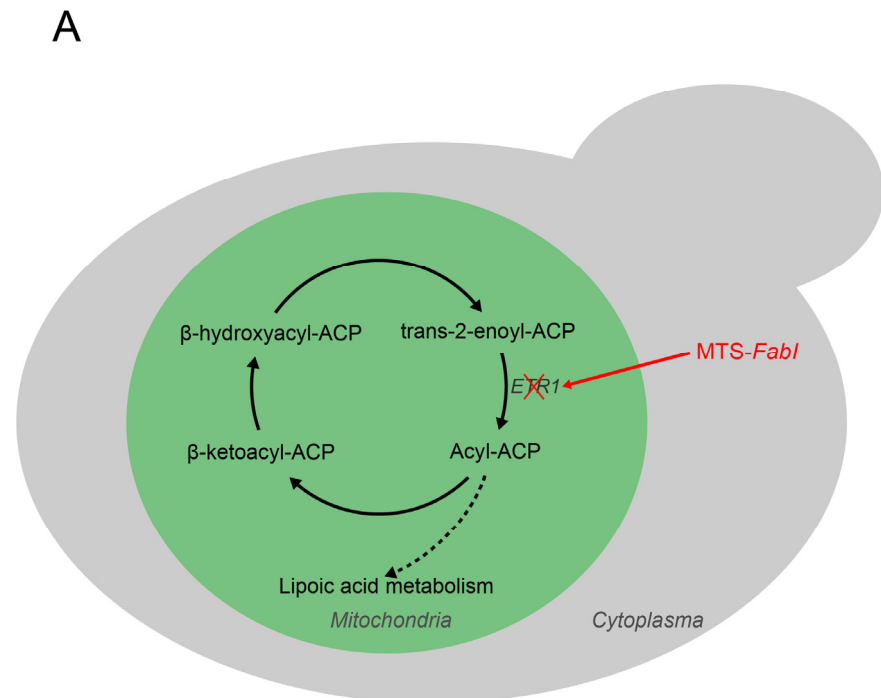
423 **Figure 1.** Characterization of MTSs via growth complementation. (A) A schematic
424 view of the growth complementation by various MTS tagged FabI proteins in the *etr1*
425 null strain. (B) Cell growth of recombinant strains harboring various MTS-*FabI*
426 plasmids. The cell density (OD600) was determined after cultivation in the non-
427 fermentable medium YPE for 72 h. Error bars represented the mean \pm s.d. of biological
428 triplicates.

429 **Figure 2.** Fluorescence microscopy of yeast strains expressing MTS tagged EGFP
430 (MTS1, MTS3, MTS4, MTS8, MTS9, MTS10, MTS12, MTS16, MTS17, and MTS18).
431 The untagged EGFP expressed in the cytosol was included as control for comparison.

432 **Figure 3.** Compartmentalization of the full pathway into the yeast mitochondria for α -
433 santalene biosynthesis. (A) Reconstructed mitochondrial α -santalene biosynthesis
434 pathway. HMG-CoA, 3-hydroxy-3-methylglutaryl-CoA; IPP, isopentenyl diphosphate;
435 DMAPP, dimethylallyl diphosphate; GPP, geranyl diphosphate; FPP, farnesyl
436 diphosphate. The 10 expression cassettes, with *ERG10*, *ERG13*, 2x*tHMGR*, *ERG12*,
437 *ERG8*, *MVD1*, *IDI1*, *ERG20*, and *SanSyn* tagged with their corresponding MTSs, were
438 assembled into two plasmids, pRS413-Mito1 (harboring genes marked in red) and
439 pRS416-Mito2 (harboring genes marked in blue). (B) Production of α -santalene in
440 recombinant CEN.PK2-1C strains harboring different combinations of plasmids.
441 Cytosol SanSyn: pRS413-*SanSyn* and pRS416; Mitochondrial SanSyn: pRS413-
442 MTS12-*SanSyn* and pRS416; Partial mitochondrial pathway: pRS413-MTS12-*SanSyn*
443 and pRS416-Mito2; Full mitochondrial pathway: pRS413-Mito1 and pRS416-Mito2;
444 Error bars represented the mean \pm s.d. of biological triplicates.

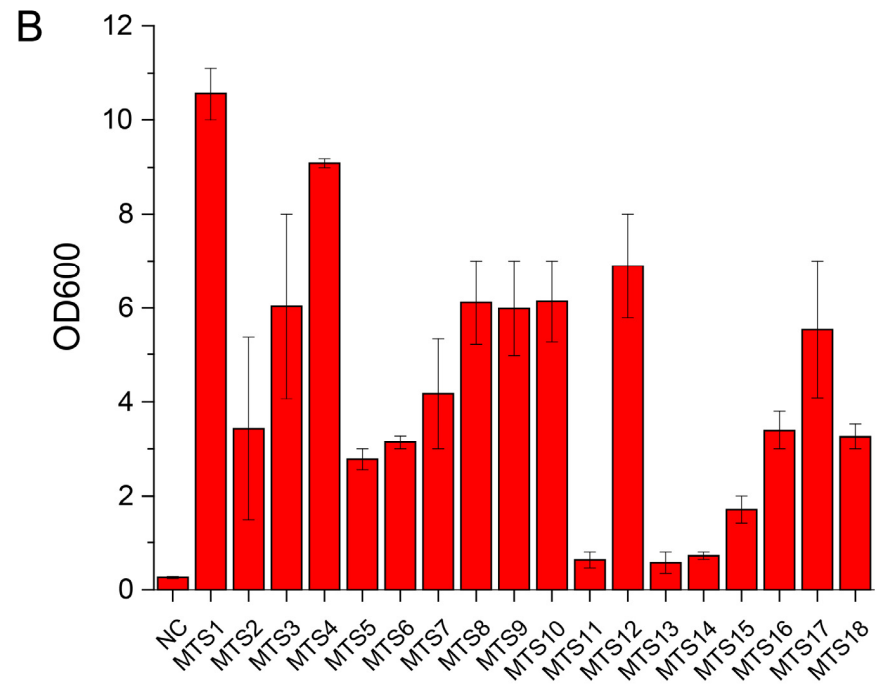
445

446 **Figure 1**

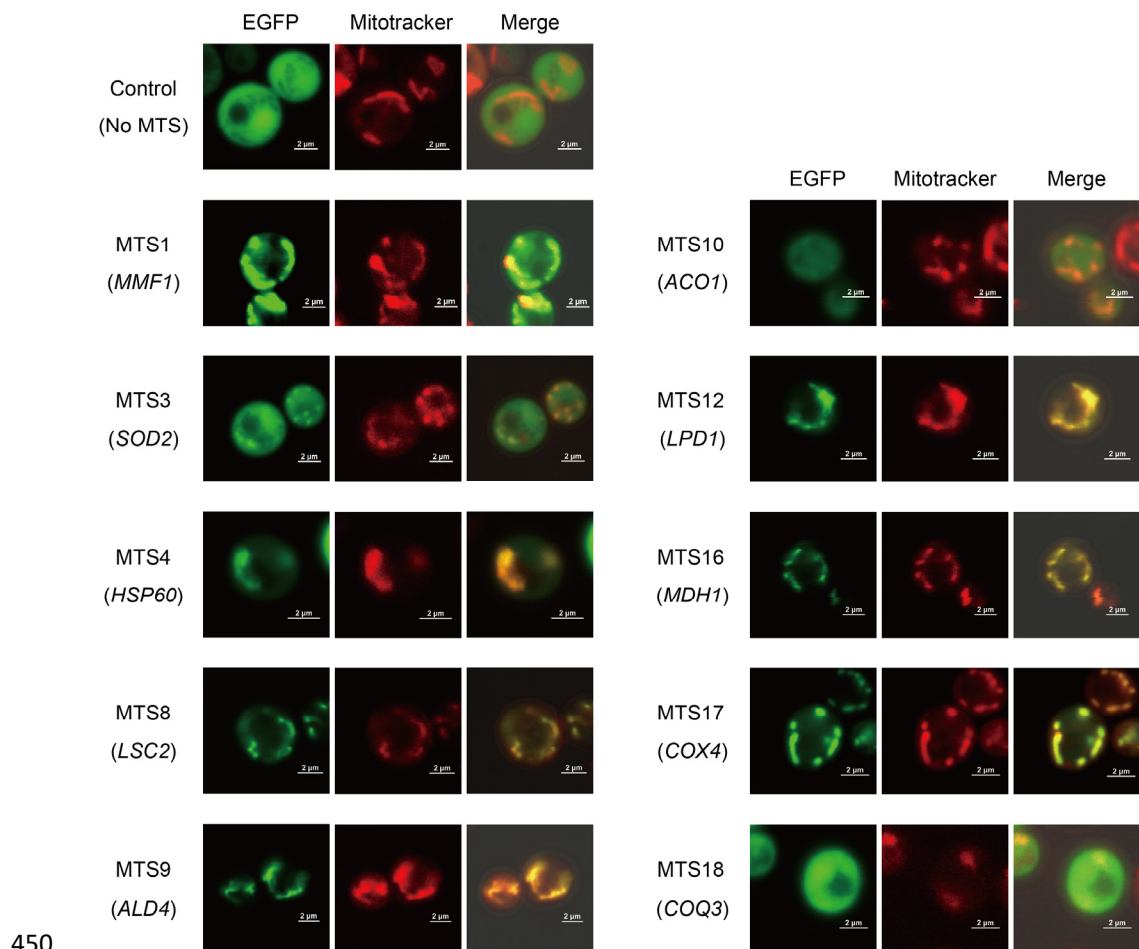


447

448



449 **Figure 2**



450

451

Figure 3